EasyChair Preprint

№ 14507

Solving the B-SAT Problem Using Quantum Computing: Smaller is Sometimes Better

Ahmad Bennakhi, Greg Byrd and Paul Franzon

September 24, 2024

Solving the B-SAT Problem Using Quantum Computing: Smaller is Sometimes Better

Ahmad Bennakhi
ECE Dept.
North Carolina State University
Raleigh, USA
aabennak@ncsu.edu

Gregory T. Byrd
ECE Dept.
North Carolina State University
Raleigh, USA
gbyrd@ncsu.edu

Paul Franzon
ECE Dept.
North Carolina State University
Raleigh, USA
paulf@ncsu.edu

***Abstract*—This paper examines the effectiveness of modern universal gate quantum computers in solving the Boolean Satisfiability (B-SAT) problem using Grover's Search algorithm. Experiments were conducted with varying configurations, including the number of shots, qubit mapping, and different quantum processors, to assess their impact on the results. The study also includes an experiment that highlights a unique behavior observed in IBM quantum processors when running circuits with a specific number of shots.**

***Index Terms*—quantum computing, B-SAT, Boolean satisfiability problem, Grover's Search, electronic design automation (EDA), conjunctive normal form (CNF), closed box testing**

I. Introduction

The applications of quantum computing on electronic design automation (EDA) is an increasingly growing field that is gaining traction as quantum processors improve by the year [1] [2]. Universal gate quantum processors are quite efficient at performing tasks that could be parallelized, and closed-box EDA testing has a lot of parallelization potential since it needs to run all possible inputs to verify the function of the digital logical unit. One way to auto-construct a closed-box digital logic unit is to lay it out as a Boolean Satisfiability (B-SAT) problem.

An early application of quantum computers is to solve the Boolean Satisfiability problem using Grover's Search algorithm [3]. Grover's search algorithm has long been hailed as one of the flagship algorithms of quantum computing [4]. Its ability to locate an item in an unstructured list has a complexity of: $O(\sqrt{n})$. That being said, quantum computers are far from proving quantum advantage. While we are still in the noisy intermediate-scale quantum (NISQ) era, various approaches from all angles are being leveraged to achieve the goal of quantum advantage. The depth of quantum circuits is usually used as an early indicator of how reliable the results will be. However, as demonstrated by the experiments in this study, you can still get both reliable results in quantum circuits with high depth and unreliable results from quantum circuits with shallower depth as well.

II. Background

A. The Boolean SAT Problem

This study explores various configurations of B-SAT circuits to identify those that yield optimal results. Our experiments are particularly relevant for quantum computing applications, especially those utilizing Grover's search algorithm to solve Boolean satisfiability problems or CNF-translated digital logic circuits.

Key variables include the number of shots, qubit mapping, and choice of quantum processor. In the CNF circuit, these variables correspond to the number of AND, OR, and NOT operators, focusing on logical rather than physical gates. A typical Boolean satisfiability equation can be expressed as:

$$\begin{aligned} f\left(x_1,\ x_2 \ldots x_n\right) = \quad & \left(x_1 \vee \neg x_2 \vee x_3 \ldots \vee x_n\right) \\ & \wedge\ \left(\neg x_1 \vee x_2 \vee x_3 \ldots \vee x_n\right) \\ & \wedge \ldots \left(x_1 \vee \neg x_2 \vee x_3 \ldots \vee x_n\right) \end{aligned} \quad (1)$$

CNF equations consist of clauses (OR combinations of literals) that are ANDed together. This structure offers flexibility, allowing CNF to represent various scenarios. The Tseytin transformation [8] optimizes CNF for converting combinational logic circuits, with any circuit convertible to CNF using De Morgan's law. A CNF circuit typically has three stages, illustrated in Figure 1: (1) input inversion (creation of literals, blue box), (2) formation of clauses using OR gates (red box), and (3) combining clause outputs with AND gates (purple box). Assuming m clauses and n variables, the proportion $\alpha = m/n$ is critical for solvability. Studies on the 3-SAT problem [5] [6] indicate a sharp drop in the probability of finding a solution beyond a critical point $\alpha_c \approx 4.267$. We ensured α remained below this threshold in all experiments.

B. Grover's Search Algorithm

The 3-SAT problem has been at the forefront when it comes to exemplifying the applications of Grover's algorithm. Grover's algorithm is composed of three components:

1) Hadamard Initiation
2) Grover Oracle
3) Amplitude Amplification

Hadamard initiation is a common initialization stage that is seen in many quantum algorithms, where all qubits are flipped to superposition. This creates an equally weighted superposition of all computational basis states, thus harnessing one of the major perks of quantum computing. The next step

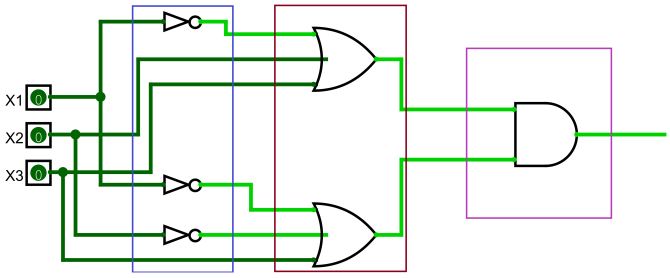

Fig. 1. Stages of a CNF circuit in digital logic form.

would be the Grover Oracle. The Grover oracle is a quantum circuit component that flips the phase of a state that satisfies a desired condition. In our experiment, the CNF equation would be translated into a Grover oracle. The last part of Grover's search algorithm is the Amplitude Amplification stage. Unlike the Grover oracle, the amplitude amplification phase is not case- nor result-dependent, meaning that the quantum circuit for the amplitude amplification remains identical for all cases and is always: $U = 2|s\rangle\langle s| - \mathbb{1}$.

After the Hadamard initiation, the algorithm works by repeatedly applying a Grover oracle and amplitude amplification for:

$$\left\lfloor \frac{\pi}{4}\sqrt{\frac{N}{m}} \right\rfloor$$

Where N is the number of entries on the list or 2^n. n is equal to the number of qubits representing the variables in the Boolean Satisfiability formula. m is the number of viable distinct solutions. Finally, the results would be recorded by measuring all qubits. By exchanging the Grover Oracle with the CNF circuit we would be constructing a Boolean satisfiability solver. The layout would can be seen in Figure 2.

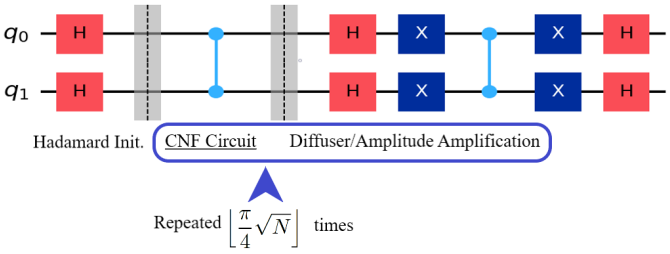

Fig. 2. In this example, the CNF circuit would be: $f(x_1, x_2) = x_1 \wedge x_2$. It should be noted that this example has only 1 distinct solution.

C. Circuit Depth

Quantum circuit depth measures the longest path from input to output, reflecting computational complexity and efficiency. Deeper circuits indicate more complex computations and increase susceptibility to errors due to prolonged qubit interactions. Parallel qubit operations do not add to the circuit depth. Minimizing circuit depth is crucial for reducing error accumulation and enhancing computation speed, which is vital given the fragility of quantum states. However, reducing depth may require more qubits or gates, complicating the trade-off between depth, gate complexity, and error correction in quantum algorithm design.

D. Shot Statistics

This section discusses the concept of 'shots' in classical and quantum computing contexts. In quantum computing, shots refer to the number of times a quantum circuit is executed or measured, playing a crucial role in analyzing outcomes and statistics. When a qubit is measured, it probabilistically collapses into a 0 or a 1, meaning that repeated executions of the same quantum circuit can yield different results due to quantum uncertainty. By running a circuit multiple times, researchers can gather statistical data from these measurements, with each execution representing one 'shot.'

The average mean of a classical operation outcome can be denoted by:

$$E[X] = \sum_{x \in 0,1} xPr[X = x] \tag{2}$$

Where $E[X]$ is the expectation value of the quantum circuit while x is meant to represent the classical measurement outcome that would be multiplied by the probability of it happening: $Pr[x]$. This can be further reduced to $Pr[X = 1]$ and result in it being just p, which is just the probability of measuring 1. When translated into quantum computing terms, the average mean formula would look something like this:

$$\begin{aligned} E[X] &= \textstyle\sum_{x\in 0,1} x\langle\hat{\mu}(x)\rangle \\ &= \langle\textstyle\sum_{x\in 0,1} x\hat{\mu}(x)\rangle \\ &= \langle\hat{M}\rangle \end{aligned} \tag{3}$$

$\hat{\mu}$ is an observable. An observable is a measurable property of a circuit, where it could be a vector or a combination of different vector outcomes. Since the expectation value is a linear function, the constant x could be moved to the inside of the $\hat{\mu}$ bracket(as seen in equation 3). This would equal the quantum expectation value of the quantum observable, as demonstrated in line 3 of equation 3. This $\hat{M}$ value is equal to the projector for the $|1\rangle$ vector, which symbolizes the probability of measuring a 1.

The variance of a classical random variable(denoted by $\mathbb{V}$), which describes the deviation around the mean, looks like the following equation:

$$\begin{aligned} \mathbb{V}[X] &= E[(X - E[X^2])^2] \\ &= E[X^2] - E[X]^2 \end{aligned} \tag{4}$$

This formula is shared by both the quantum and classical aspects, but what they differ in is the way that the expectation value squared($E[X^2]$) is reached. The difference is demonstrated in Table I. At the end of the quantum path, we can see that the expectation value squared is equal to the observable operator matrix squared. By combining both sides of the variance equation, we can induct that:

TABLE I
AN OUTLINE OF THE CLASSICAL AND QUANTUM EXPECTATION VALUE SQUARED

Classical $E[X^2]$	Quantum $E[X^2]$
$E[X^2] = \sum_{x\in 0,1} x^2 Pr[X=x]$ $= 0Pr[X=0] + 1Pr[X=1]$ $= p$	$E[X^2] = \sum_{x\in 0,1} x^2 Pr[X=x]$ $= \sum_{x\in 0,1} x^2 \langle\hat{\mu}(x)\rangle$ $= \langle\sum_{x\in 0,1} x^2 \hat{\mu}(x)\rangle$ $= \langle\hat{M}^2\rangle$

$$\begin{aligned}\mathbb{V}[X] &= \langle\hat{M}^2\rangle - \langle\hat{M}\rangle^2 \\ &= p - p^2 \\ &= p(1-p)\end{aligned} \tag{5}$$

The **chi-square**, denoted by χ^2, is a statistical parameter that measures how close model data is when compared to observed data. It is formulated in the following equation:

$$\chi_c^2 = \frac{(O_i - E_i)^2}{E_i} \tag{6}$$

Where O represents the observed values, E_i represents the expected values, and c denotes the degrees of freedom. The larger the disparity between the observed and model values, the larger the χ^2 value is. In other words, the smaller χ^2 is the better the model/experiment appears to be. More detailed information can be found regarding this subsection at [9].

Number of Shots: A single measurement(shot) of a quantum circuit has a probability of measuring a particular observable x would be written as:

$$\Pr[X = x] = \langle\hat{\mu}(x)\rangle \tag{7}$$

The average over all the random outcomes measured would be denoted as S and formulated in the following way:

$$S = \frac{1}{M}\sum_{m=1}^{M} X_m \tag{8}$$

Where the first outcome is X_1 and the last measurement outcome is X_M. The number of shots measured here is M. Equation 5 is applicable in the context of the number of shots and by combining it with equation 4, we can induct that:

$$E[X_m] = E[X] = p \qquad \forall m \in \{1, ..., M\} \tag{9}$$

As stated earlier, the expectation value is linear functional and is even utilized in equation 4. This property can be also used to derive the distributed expectation value, as seen in the following equation:

$$E[aX_m + bX_n] = aE[X_m] + bE[X_n] \qquad \forall m, n \quad a, b \in \mathbb{C} \tag{10}$$

Again, when using equation 4 to come up with the variance of a distributed random variable system(such as the quantum uncertainty), we can infer that the variance would be equal to:

$$\mathbb{V}[aX_m + bX_n] = a^2 E[X_m] + b^2 E[X_n] \qquad \forall m, n \quad a, b \in \mathbb{C} \tag{11}$$

Following on from equation 9 and combining it with equation 8, we can assume that the variance of the mean for quantum systems can be laid out in the following way, given M number of shots taken into account:

$$\begin{aligned}\mathbb{V}[S] &= \mathbb{V}[\tfrac{1}{M}\sum_{m=1}^{M} X_m] \\ &= \tfrac{1}{M^2}\sum_{m=1}^{M} \mathbb{V}[X] \\ &= \tfrac{1}{M}\mathbb{V}[X] \\ &= \tfrac{p(1-p)}{M}\end{aligned} \tag{12}$$

This would indicate that in an ideal quantum computing system; The more measurements or shots, the smaller the standard deviation and variance becomes. In other words, you can suppress quantum projection noise with enough shots. This could be demonstrated in Figure 3.

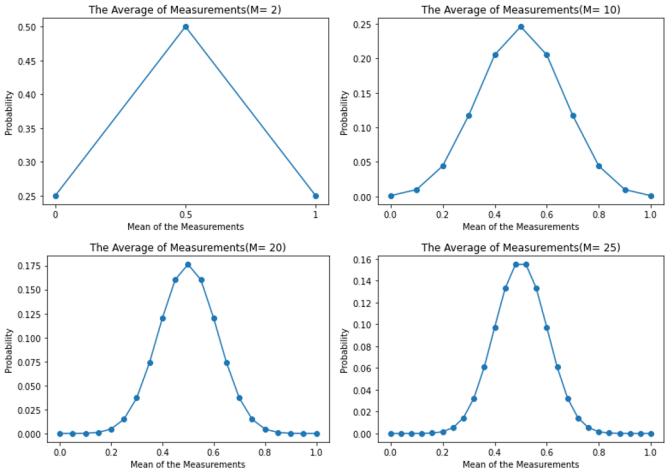

Fig. 3. Variance of Random Classical Variable Vs. Probability to Measure 1. The probability of yielding outlier mean measurements decreases as the number of shots is increased. This should be an indicator that the variance should decrease as the number of shots is increased.

III. METHODOLOGY

A. B-SAT Experiment

The experiment begins by constructing a dimacs file in CNF. A dimacs file is a text file that is used to describe a Boolean satisfiability problem in various forms. The dimacs file is parameterized by the number of variables, AND gate logical operators, OR gate logical operators, and then a proportion of literals randomly get a NOT gate applied to them. In the context of our study, the number of AND and OR gates would translate into literals and clauses in the following way:

$$\#\text{ANDs} = \#\text{Clauses} - 1 \tag{13}$$

$$\#\text{ORs} = \sum_{clause} (\#\text{Literals} - 1) \tag{14}$$

TABLE II
A SAMPLE OF THE EXECUTED CIRCUITS IN TERMS OF PARAMETERS

n=3 B-SAT	3 AND gates	6 OR gates	30% NOT gate application
			50% NOT gate application
			70% NOT gate application
		7 OR gates	30% NOT gate application
			50% NOT gate application
			70% NOT gate application
		8 OR gates	30% NOT gate application
			50% NOT gate application
			70% NOT gate application
	4 AND gates	8 OR gates	30% NOT gate application
			50% NOT gate application
			70% NOT gate application
		9 OR gates	30% NOT gate application
			50% NOT gate application
			70% NOT gate application
		10 OR gates	30% NOT gate application
			50% NOT gate application
			70% NOT gate application

The CNF equation was checked for duplicates, restarting the random allocation of NOT gates if any were found. After 100 attempts, duplicates were allowed. B-SAT problems are classified by the number of variables/qubits, n, used in the quantum circuit. The pattern used by the DIMACS CNF constructor is shown in Table II, with the number of DIMACS files per configuration listed in Table III.

TABLE III
NUMBER OF DIMACS FILES GENERATED PER CONFIGURATION

SAT Configuration	Number of dimacs Files Generated
n=3	64 files
n=4	325 files
n=5	709 files
n=6	880 files

The dimacs file is then translated into a quantum circuit with the intended adjustments made. The constructed circuit is then sent to IBM's quantum processors to be run according to the specified number of shots. The whole experiment is coded in Python and Qiskit, IBM's quantum computing library. The stages of this experiment are visually summarized in Figure 4.

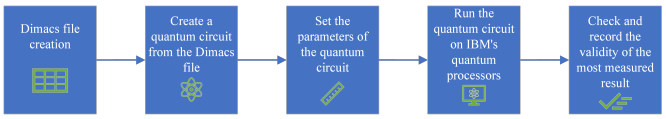

Fig. 4. A brief summarization of the experimental procedure

The quantum circuits representing the Boolean SAT digital logic are run on three of IBM's quantum processors: Quito, Lagos, and Toronto. The processor specifications are listed in Table IV. Each circuit is executed 10 times(with the specified number of shots) and at the end of each execution, the result with the highest occurrence is tested on the actual equation to determine whether it is a valid solution or not.

Qubit mapping was performed using a library called "Mapomatic" [7]. Mapomatic is a library of qubit mapping functions that was developed by a group of researchers at IBM Quantum. It should be noted that the qubit mapping algorithm is not deterministic, meaning that the mapping procedure would sometimes yield slightly different mapping layouts. That being said, the difference is very slight and rarely exceeds 10 in quantum circuit depth. All quantum circuits are transpiled with $optimization\_level = 3$ this would automatically apply a heavy circuit mapping optimization pass, hence a mapped circuit would have a double layer of qubit mapping passes applied.

TABLE IV
QUANTUM PROCESSOR SPECIFICATIONS

Processor	*Qubits*	*QV*	*Median Readout ERR*	*Median CNOT ERR*
Quito	5	16	4.250e-2	1.012e-2
Lagos	7	32	1.667e-2	7.135e-3
Toronto	27	32	1.910e-2	1.009e-2

∗The error rates listed were taken according to the calibrations taken on the 7th of April 2023

B. Shots Experiment

This experiment is a branch-out experiment motivated by the unexpected results observed in the experiment described in section III-A. Our experiment begins by recording the Error Per Clifford(EPC) data of a single physical qubit, in one of IBM's superconducting quantum processors, by using Qiskit's Standard Randomized Benchmarking library functions [10]. After performing these single qubit experiments, a bundle of quantum circuits would be constructed, using the same library, that would range from a certain quantum circuit depth to another. Each of the 1-qubit data collection experiments has to be performed within a relatively short time window before each multi-qubit standardized random benchmarking experiment, otherwise a large disparity would be noticed. The 1-qubit data is used as the expected values E_i in equation 6.

Given a specified seed value, the randomized circuits would always generate the same "random" standard benchmarking circuit. The depth of each Clifford is gradually increased in the bundled multi-qubit experiments, resulting in a range of circuits rather than just a single circuit depth. This variation in Clifford gate length is required by Qiskit's standard randomized benchmarking functions to analyze the EPC's spread by calculating the variance, while also mapping the divergent behavior that would be demonstrated in the reduced chi-squared of the EPC behavior. These same experiments have been performed with different amounts of qubits in a circuit, which did affect the produced random circuit depth. The main variable in our experiments that the whole experiment was built around is the number of shots performed in each multi-qubit benchmarking execution. A summary of the experimental procedure can be seen in Figure 5.

This experiment's main objective is to examine the effect that the number of shots would have concerning the number of qubits under a circuit depth that would not likely result in random noise(49-156) from the effects of having a higher variance effect(as demonstrated in Figure 3). The time of each

experiment after quantum processor calibration was recorded but not included in the results due to its irrelevance to the analysis.

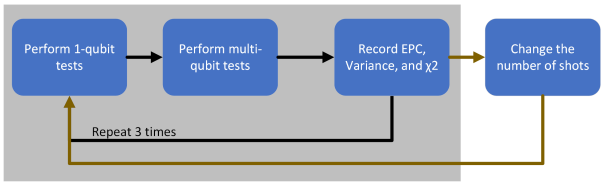

Fig. 5. This is a figure that summarizes our experimental procedure. The black arrows are to be repeated 3 times per cycle, while the olive-colored lines are performed once per cycle.

IV. Results

A. B-SAT Experiment

1) Three Qubits(n=3): Our first experiment in this subsection runs two configurations of the three variable/qubit B-SAT problem. All circuits are set to n=3, meaning that the number of variables in the circuit is 3. All of the circuits were run with and without reapplying qubit mapping. Both executions have been set to 1024 shots per circuit execution. The results can be seen in Figure 6. The "Success Score" marking the Y-axis indicates how well the top result of the 10 quantum computer executions faired; 0 means that none of the top measurements in the quantum circuit runs yielded correct answers and 1 means that all of the top measurements yielded correct answers. Due to the very simple nature of the circuit, the results are mostly perfect with few dips in fidelity. It is also noticeable that the qubit mapping optimization seems to aggravate the drop in the success score.

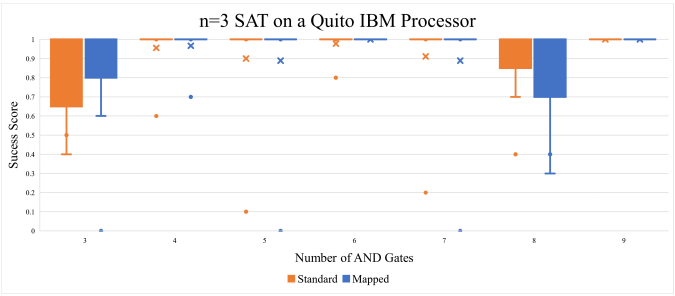

Fig. 6. The n=3 SAT results on Quito gave us almost perfect answers with few outliers here and there

There was one unexpected trend that came out of the n=3 SAT experiments. The circuit depth of the unmapped quantum circuits yielded better results as the depth goes above the 30s. This could be due to coherent errors, as they have a similar pattern of oscillating in magnitude as more operations are applied to a qubit. Generally, circuit depth is seen as something that should be minimized as much as possible, but in this case, it has shown to be a positive marker seen in Figure 7. Qubit mapping in the n=3 SAT circuit did not improve the results as can be seen in Figure 8. Qubit mapping also resulted in higher average circuit depth.

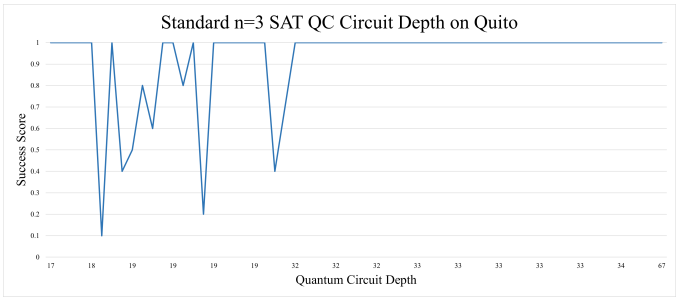

Fig. 7. Circuit depth seems tied to more positive results with the unmapped n=3 B-SAT.

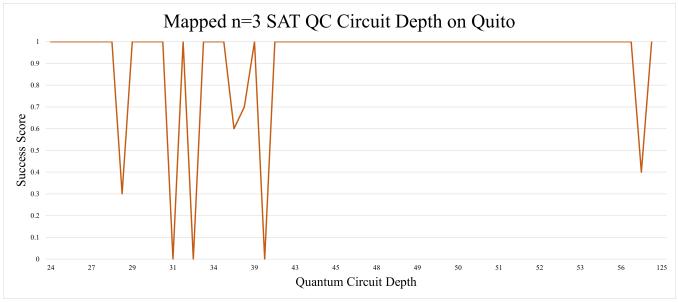

Fig. 8. Qubit mapping did not improve the n=3 SAT results by much.

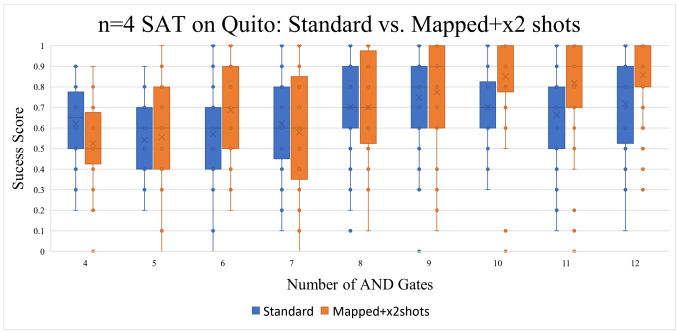

Fig. 9. Increasing n to 4 shows a noticeable decline in the success score, but some improvement with qubit mapping and increased shot count per execution.

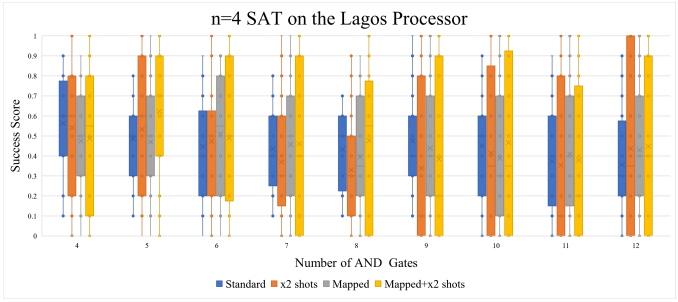

Fig. 10. Doubling the shot count and using qubit mapping resulted in an aggravated Success Score on Lagos.

2) Four Qubits(n=4): This subsection explores the impact of qubit mapping and varying shot counts on quantum circuits with four variables, as well as a comparison between the Quito and Lagos quantum processors. Upon increasing the variables to $n = 4$, a significant drop in fidelity is observed (Figure 9) compared to $n = 3$ (Figure 6). Applying qubit mapping and doubling the shot count to 2048 improved results, especially with more AND gates. Interestingly, the Lagos processor, despite having more qubits and lower error rates (Table IV), yielded a lower "Success Score" compared to Quito. Qubit mapping and increased shots enhanced results on Quito (Figure 9), but not as effectively on Lagos (Figure 10). On Lagos, doubling the shots without qubit mapping resulted in worse outcomes, with an increase in zero scores.

Circuit depth analysis on Quito revealed a negative impact on fidelity for the n=4 SAT circuits, with deeper circuits yielding poorer results (Figure 11). In contrast, Lagos showed no significant depth-related trends, except for a slight increase in correctness at higher depths, possibly due to an increase in OR gates (Figure 12).

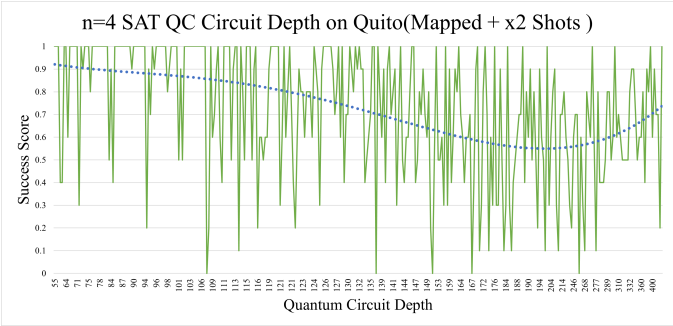

Fig. 11. The dotted blue line indicates a polynomial aggregation of the experimental results on Quito.

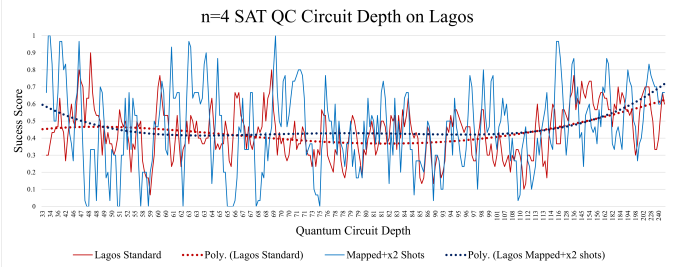

Fig. 12. No noticeable pattern in depth aspect for the n=4 SAT runs on Lagos.

3) Five Qubits(n=5): The number of shots here has been adjusted to 4096 in all executions. As seen in Figure 13, both cases had a success rate that resembles the probability of random chances of success. However, we were surprised to find a particular trend when analyzing the success score against the quantum circuit depth. Figure 14 is a polynomial of order 6 aggregate line of the standard n=5 SAT Quito experiments. Quantum circuits with a depth over 1000 have shown to have a score approaching 0.9. The effect is also applicable to lower polynomial aggregation lines that are. This prompted us to cross-examine it with the random chance of success in the "Further Analysis" subsection.

We performed n=5 experiments on another quantum processor, Kolkata, using IBM's updated runtime library. Unfortunately, the results resembled as well. The experiments were repeated while setting the resilience level to 1, which did raise the chances of success by only 4-5%. To verify our modus operandi, we also ran some of the lower depth n=5 circuit experiments on IBM's mock quantum processor "Fake Kolkata", which gave us almost perfect results(these mock processors have some simulated noise applied to them).

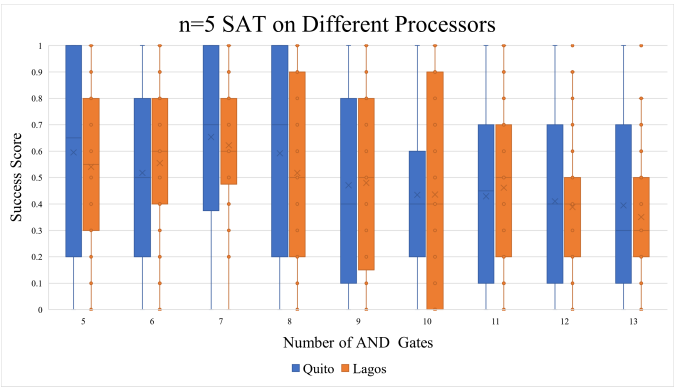

Fig. 13. Both Quito and Lagos seem to have produced similar results, which would be interpreted as noise when factoring in the random chance of success

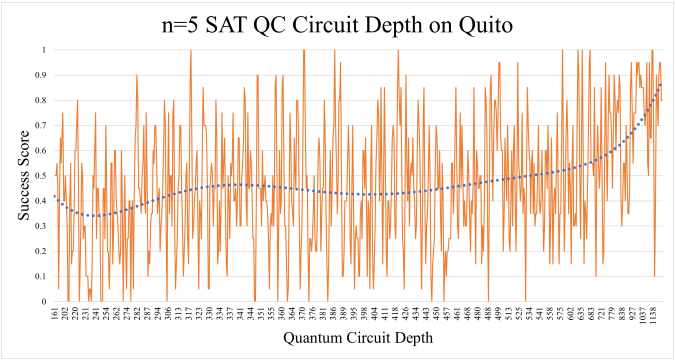

Fig. 14. In this case, the n=5 SAT experiments indicate that high circuit depth is caused by a higher number of OR gates, which results in a higher probability of random success

4) Six Qubits(n=6): For the n=6 SAT problem, we used IBM's Toronto quantum processor to examine if it would keep up with the increasing amounts of qubits required. The number of AND gates in these quantum circuit runs had no clear pattern (as seen in Figure 15), other than they were approximately on level with the random noise success rate: 46%(more details in the "Further Analysis" section). The number of shots ran on Toronto was adjusted to 8192 to compensate for the increased size of the state vector. No comparison experiment was executed other than the standard one for the n=6 SAT.

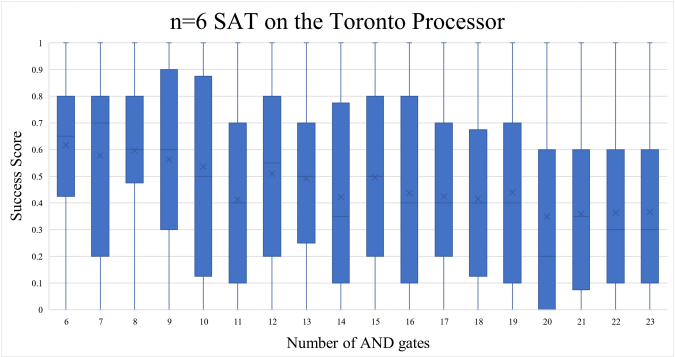

Fig. 15. As the number of AND gates increases, the results drop to just noise level integrity

5) Further Analysis: This subsection will discuss points that have not been brought up in the previous subsections and the possible reasoning behind the results. The vast majority of CNF equations have more than 1 valid solution, and this section aims to examine this span of valid/satisfiable answers. According to the n=5 SAT and n=6 SAT circuits that have been generated for this study, this span is very predictable. As seen in Figure 16. The ratio of OR:AND gates is what decides how big the span of satisfiable solutions is. As the number of AND gates increases, the ratio gets lower thus pulling the success score down. This effect can be slightly seen in the n=5 SAT executions on Quito (Figure 13). The effect is also noticeable even on the n=4 Lagos graph in Figure 10), but not the n=4 Quito graph in Figure 9.

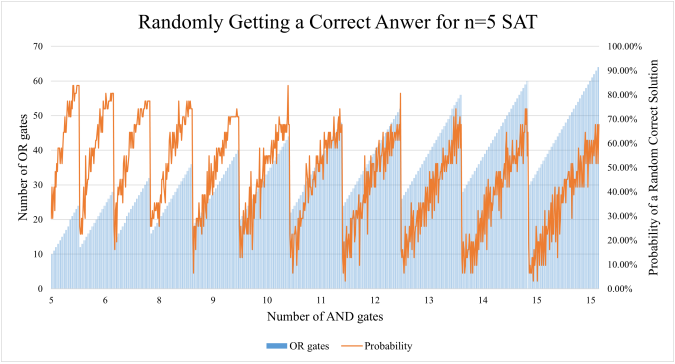

Fig. 16. The ratio of OR:AND gates is what decides how big the span of satisfiable solutions

When comparing the general experimental results with the probabilistic rates (Table V), the picture becomes clearer. modern-day quantum computers could handle n=3 SAT and n=4 SAT problems adequately enough, but when raising n to 5 and above, they start to yield random noise results. The n=4 SAT results were only significantly higher than the probabilistic trend in the case of the Quito (mapped+x2 shots). The rest of the n=4 SAT implementations were close to the probabilistic stats in terms of average, median, and correlation. Trying to solve the problem on a larger quantum processor such as Lagos or Toronto did not give us better results, even though their median gate and readout error rates (see Table IV) were less than the smaller Quito processor.

TABLE V
STATISTICAL COMPARISON BETWEEN THE EXPERIMENTAL RESULTS VS. PROBABILISTIC CHANCE OF RANDOM SUCCESS

Quantum Processor	**Probablistic**
n=3 SAT on Quito Average: 93% Median: 100%	n=3 SAT Average: 39% Median: 43%
n=3 SAT Correlation: -0.5311	
n=4 SAT on Quito (Mapped+x2 Shots) Average: 73% Median: 80%	n=4 SAT Average: 42% Median: 40%
n=4 SAT Correlation: -0.4132	
n=5 SAT on Quito Average: 50% Median: 50%	n=5 SAT Average: 46% Median: 48%
n=5 SAT Correlation: 0.4852	
n=6 SAT on Toronto Average: 44% Median: 40%	n=6 SAT Average: 44% Median: 45%
n=6 SAT Correlation: 0.6176	

Moreover, the correlations are quite clear (see Table V) regarding how much the results are affected by the random probability's safety umbrella. It should be noted that circuits with more OR gates resulted in larger quantum circuit depth, while the number of AND gates did not have a noticeable effect on the depth. The proportion of NOT gates in the circuits did not have any significant effect on the results, hence not mentioned in the previous subsections.

We have no conclusive evidence to explain the cause of the larger variance in the n=4 circuits, especially in Lagos, and this has led us to email IBM Quantum regarding this matter. They explained that the cause of this behavior is due to a miscommunication on whether more shots are coming and that this behavior is both hardware and firmware version specific. We were also assured by IBM Quantum that the issue should be patched soon in the next backend upgrade. For more information regarding the effect that the number of shots imposes, please refer to the results of the shots experiment(subsection IV-B).

B. Shots Experiment

The results proved what we suspected from the B-SAT experiment, which is that the number of shots did affect the results in unusual ways. To be precise, the variance and fidelity did not peak at the lowest number of shots. As seen in Figure 18, the χ^2 on the Kolkata quantum processor shows a predictable pattern by peaking at particular numbers of shots as the number of qubits increased. When the number of qubits is 5, the χ^2 peaks at 2000 shots, and when the number of qubits is increased to 6, the χ^2 peaks at 4000 shots. The pattern persists with the 7-qubit circuits where the χ^2 peaks at 6000 shots. The 8-qubit circuit verified the previous pattern by the χ^2 showing a spike in χ^2 at the 8000 shot mark. It also showed signs of obeying the conceptual rules demonstrated in subsection II-D by having a higher variance when the number of shots is set to the lowest setting in our experiments.

Kolkata also showed these spikes in variance, but they peaked in different number of shots than the χ^2 as seen in Figure 18. The spike in variance seems to be set at 6000 shots when the number of qubits in the circuits is 7 and 8. Otherwise, the spike in variance followed the χ^2 pattern when the number of qubits is 5. The other quantum processor, Cairo, displayed a similar spike in variance and χ^2 that repeats in the same number of shots and qubits(as seen in figure 17). This would lead us to speculate that this occurrence is not tied to a single quantum processor.The spike also appears on the Hanoi quantum processor at 4000 shots, rather than 2000, when running the 5-qubit circuit (Figure 17).

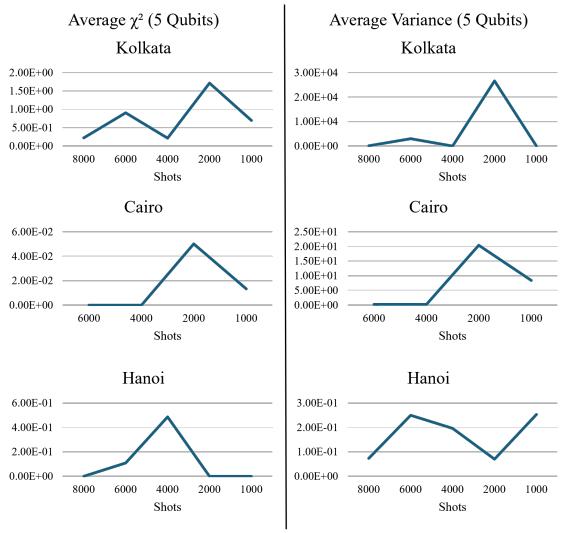

Fig. 17. The number of shots across 3 quantum processors yields unexpected results deviating from the mathematical model. Fidelity(measured by χ^2) drops are also oddly linked to the number of qubits (left).

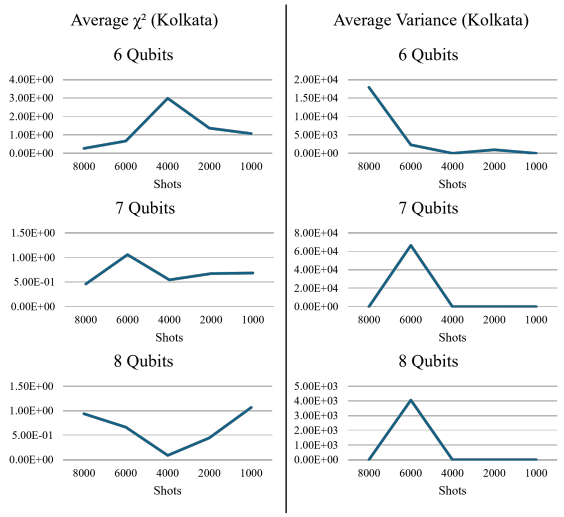

Fig. 18. Experiments on Kolkata show a predictable fidelity loss spike shifting left with each qubit increment (left). Variance spikes occur at 8000 and 6000 shots on 5+ qubit circuits (right).

V. Conclusion

After performing numerous experiments, we have reached several key points:

- Quantum volume and declared error rates of a quantum processor were not indicators of how well it performed in our B-SAT experiments. Quito, the quantum processor with fewer qubits, lower quantum volume, higher median readout and CNOT error rate than Lagos, yielded noticeably better results in the n=4 case.
- Increasing the number of shots did not result in a lower result variance, as it increased the variance in a certain higher number of shots. According to IBM, the cause of this issue is the firmware on their quantum processor. This hardware-firmware issue has affected numerous quantum experiments, not just our B-SAT experiment.
- The extra layer of qubit mapping almost always resulted in improved average results.
- A bigger circuit depth does not always imply worse results (at least not for an SAT circuit), as it sometimes gives us better results even when taking the random chance of success into account.
- The quantum processors experimented on performed adequately on the n=3 and n=4 SAT circuits, but the results declined to noise level for the n=5 SAT and n=6 SAT.

Acknowledgment

The authors would like to thank John Streck for managing the reservations used in this study. We also acknowledge the Kuwait Institute for Scientific Research for their financial support.

References

[1] Alwin Zulehner and R. Wille, Introducing Design Automation for Quantum Computing. Springer Nature, 2020.

[2] I. Turtletaub, G. Li, M. Ibrahim, and P. Franzon, "Application of Quantum Machine Learning to VLSI Placement," Proceedings of the 2020 ACM/IEEE Workshop on Machine Learning for CAD, Nov. 2020, doi: https://doi.org/10.1145/3380446.3430644.

[3] C. Zalka, "Grover's quantum searching algorithm is optimal," Physical Review A, vol. 60, no. 4, pp. 2746–2751, Oct. 1999, doi: https://doi.org/10.1103/physreva.60.2746.

[4] N. J. Cerf, L. K. Grover, and C. P. Williams, "Nested quantum search and NP-complete problems," arXiv [quant-ph], 1998.

[5] Gabor, T., Zielinski, S., Feld, S., Roch, C., Seidel, C., Neukart, F., Galter, I., Mauerer, W. & Linnhoff-Popien, C. Assessing solution quality of 3SAT on a quantum annealing platform. *Quantum Technology And Optimization Problems: First International Workshop, QTOP 2019, Munich, Germany, March 18, 2019, Proceedings 1*. pp. 23-35 (2019)

[6] Mézard, M. & Zecchina, R. Random k-satisfiability problem: From an analytic solution to an efficient algorithm. *Physical Review E*. **66**, 056126 (2002)

[7] Nation, P. & Treinish, M. Suppressing Quantum Circuit Errors Due to System Variability. *PRX Quantum*. **4**, 010327 (2023,3), https://link.aps.org/doi/10.1103/PRXQuantum.4.010327

[8] Tseitin, G. On the complexity of derivation in propositional calculus. *Automation Of Reasoning: 2: Classical Papers On Computational Logic 1967–1970*. pp. 466-483 (1983)

[9] Qiskit-Community, "Qiskit-Community/QGSS-2023: All things qiskit global summer school 2023: Theory to implementation - lecture notes, Labs and Solutions,", https://github.com/qiskit-community/qgss-2023

[10] "Randomized benchmarking" Randomized Benchmarking-Qiskit Experiments 0.5 0.5.4 documentation, https://qiskit.org/ecosystem/experiments/manuals/verification/randomized_benchmarking.html (accessed Nov. 7, 2023).